AJAE

Open Access

Vol. 13, No. 3, pp. 186-195, September 2019
doi: https://doi.org/10.5572/ajae.2019.13.3.186
ISSN (Online) 2287-1160, ISSN (Print) 1976-6912

Research Article

The Use of LIF-based Instrument with 405 nm for Real-time Monitoring of Aerosolized Bio-particles

Sung Nyo Yoon*, Jaekyung Lee, Duckho Kim, Hyun Sang Yoo, Kyung Yool Min, Min Cheol Kim

Analytical Instrumentation Research Institute, Samyangchemical Co., Ltd.
593, Anyang-ro, Manan-gu, Anyang-si, Gyeonggi-do, Republic of Korea

***Corresponding author.**
Tel: +82-31-470-3826
E-mail: 9918348@samyangchem.com

Received: 18 June 2019
Revised: 3 September 2019
Accepted: 4 September 2019

ABSTRACT Bio-aerosols can affect public health depending on the origin of bio-particles (bacteria, virus etc.). Here, we attempted to assess the applicability of laser-induced fluorescence (LIF) instrument with 405 nm to real-time monitoring of bacteria and virus-containing aerosols. For the purpose, the LIF-based BDS (Bio-aerosol Detection System) was used. The bio-particle monitoring of the BDS is based on fluorescence signals from two wavelength ranges [short wavelength range (SWR): 430–550 nm & long wavelength range (LWR): 500–600 nm] and the scattering signal. Firstly, auto-fluorophores (NADH, riboflavin, tyrosine, tryptophan) were tested to expect the monitoring ranges of the BDS for the auto-fluorophores. NADH and riboflavin showed fluorescence signals from two wavelength ranges, and the fluorescence efficiency of NADH was higher in the SWR than in the LWR and that of riboflavin was reversed. While tyrosine and tryptophan showed negligible fluorescence signals from two wavelength ranges as expected. Next, the lyophilized powders of *Bacillus subtilis* (BS), virus vaccines [ND (Newcastle Disease), IB (Infectious Bronchitis)] and the bacteriophage *MS2* were tested to investigate the monitoring ranges of the BDS for the bio-particles. Individual virus and bacteriophage have been expected no fluorescence signals because of the absence of NADH and riboflavin fluorescing by 405 nm. Nonetheless, all the tested samples showed the fluorescence signals in the size range of 2 to 15 μm, generally known as bio-aerosol size. Considering that atmospheric virus particles are released through the respiratory organs of their hosts, just as virus vaccines from chicken embryo and *MS2* from *E. coli*, it can be thought in turn that the BDS can also monitor bio-aerosols including virus as well as bacteria. Taken together, we suggests that the BDS, LIF-based instrument with 405 nm, is applicable for real-time monitoring of virus-containing aerosols as well as other bio-aerosols by counting the fluorescence particles and resolving their particle sizes.

KEY WORDS Bio-aerosol, Bio-particle, LIF (Laser-induced fluorescence), Auto-fluorophore, Fluorescence signal, Scattering signal, Real-time monitoring, NADH (Nicotinamide Adenine Dinucleotide, reduced)

1. INTRODUCTION

Bio-aerosols can serve as a transmission vehicle for numerous and diverse types of non-pathogenic or pathogenic bio-particles including virus, bacteria, and fungi (II *et al.*, 2017; Alonso *et al.*, 2014; Cowling *et al.*, 2013; Li *et al.*, 2004). Pathogenic bio-particles are associated with a wide range of adverse public health impact and

Copyright © 2019 by Asian Journal of Atmospheric Environment
This is an open-access article distributed under the terms of the Creative Commons Attribution Non-Commercial License (http://creativecommons.org/licenses/by-nc/4.0/), which permits unrestricted non-commercial use, distribution, and reproduction in any medium, provided the original work is properly cited.

are mainly infected through respiratory tract (Douwes *et al.*, 2003). Thus, it is important to monitor the bio-aerosols of the respiratory aerosol fraction that may contain pathogens in real-time to reduce the damage of life and property. However, traditional approaches involving culture and genetic technologies are not appropriate because they require days or complex procedures to get the results (Denoya, 2016). There have been many efforts to overcome the disadvantages of traditional approaches by adopting optical instruments (Denoya, 2016; Wei *et al.*, 2016; Choi *et al.*, 2014; Huffman *et al.*, 2009). One of them is the laser-induced fluorescence (LIF) instrument. The principle is that bio-particles fluoresce when subjected to ultraviolet light (UV), which is not common response for non-biological particles, resulting in discrimination of bio-particles against non bio-particles in real time. The fluorescence of bio-particles is due to intrinsic auto-fluorophores. The predominant auto-fluorophores found in bio-particles are the amino acids, which are the fundamental building blocks of peptides and proteins. Of the 20 candidate amino acids, only tyrosine, phenylalanine, and tryptophan are fluorescent (due to their aromatic components), and have absorption maxima between 260–280 nm and fluorescence maxima between 280–360 nm (Fennelly *et al.*, 2018). Coenzymes are further category of the auto-fluorophores that contribute to atmospherically relevant bio-aerosol fluorescence. Coenzymes, such as NADH (Nicotinamide Adenine Dinucleotide, reduced) and NADPH (Nicotinamide Adenine Dinucleotide Phosphate, reduced), are typically present in many bio-particles. These coenzymes absorb maxima between 340–360 nm and fluoresce maxima between 440–470 nm (Fennelly *et al.*, 2018). Riboflavin is also an important contributor to the auto-fluorescence of bio-particles. Its absorption and fluorescence maxima are between 450–488 nm and between 520–560 nm, respectively (Fennelly *et al.*, 2018; Pan, 2015). Depending on the type of microorganisms such as bacteria, fungal spores and viruses, the composition of auto-fluorophores is different. The common auto-fluorophores of these bio-particles are amino acids like tryptophan and tyrosine, while NADH and riboflavin are absent in individual virus and almost negligible in fungal spore (Hill *et al.*, 2013). Nonetheless, one reported that the tested viruses fluoresce between 475–500 nm when excited at 405 nm, which was considered to be influenced by the culture medium (Pan, 2015). This means that the proliferation and release processes of virus particles, as well as their innate auto-fluorophores composition, also have a significant impact on fluorescence monitoring, especially for airborne bio-particles. Others also demonstrated the instrument-specific such as laser intensity and signal collection efficiency as well as the excitation wavelength in fluorescence detection (Saari *et al.*, 2014). The most well-known real-time LIF instrument is UVAPS (Ultraviolet Aerodynamic Particle Sizer™, TSI Inc., St. Paul, MN, USA) The instrument uses a 355 nm laser source and detects the fluorescence of aerosol particles within the size range of 0.5–15 μm. The performance of the UVAPS against bacteria, fungal spores, and auto-fluorophores (NADH and riboflavin) has been reported (Agranovski *et al.*, 2004; Agranovski *et al.*, 2003). Another commercial version of the instrument is BioScout (Environics Ltd, FI-50101, Mikkeli, Finland) which has 405 nm laser source and the size range of 0.5–10 μm. Although its excitation wavelength are different from that of UVAPS, it has been reported that the performance against bacteria, fungal spore, and auto-fluorophores is virtually no difference from UVAPS (Saari *et al.*, 2014). Bacteria or fungal spores are mostly used to assess the performance of the LIF instrument for bio-aerosol monitoring, however, virus particles are rarely used, despite being easily infected through the air. The study on the applicability of the LIF instrument with 405 nm to monitoring bio-aerosols including virus particles has not been done well. In the study, we demonstrate the real-time monitoring capability of the LIF instrument with 405 nm using aerosolized bacteria and virus particles. For the purpose, we used the LIF instrument with 405 nm, BDS (Bio-aerosol Detection System) (Yoon *et al.*, 2018). Monitoring was performed within the two kinds of aerosol chambers: One is for the fluorescence efficiencies and monitoring ranges, the other for real-time monitoring. To our knowledge, this represents the first study on the performance of the LIF instrument with 405 nm by monitoring aerosolized bio-particles including virus vaccines or the bacteriophage *MS2*, as well as bacteria.

2. MATERIALS AND METHODS

2.1 Description of the Instrument (BDS)

BDS (Bio-aerosol Detection System, Samyangchemical Co., Ltd, Korea) was based on the BAMS (Biological Aerosol Monitoring System) developed with the authority of the South Korean government, Agency for Defense

Development, using LIF technology for military requirement. A detailed description of the BDS has been given elsewhere (Yoon *et al.*, 2018; Choi *et al.*, 2014). Here, a brief description will be given. The BDS consists of a detector and a collector. In the study, only the detector of the BDS is used, and is referred to as the BDS. It consists of a concentration module and a monitoring module (Fig. 1). The concentration module is designed to enrich particles of 1 to 10 μm which ranges to the respiratory aerosol fraction. Next, the enriched particles pass through the monitoring module to distinguish bio-particles from non bio-particles. The principles of monitoring is based on fluorescence signals from two wavelength ranges (SWR: 430–550 nm, LWR: 500–600 nm) and the scattering signals emitted from particles by 405 nm. It counts as bio-particles when the fluorescence signals are emitted simultaneously, and as non bio-particles when the only scattering signals are emitted. In addition, the scattered signals are measured to determine the particle sizes. The optical properties of the BDS are similar to those of an OPC (Optical Particle Counter). Particle sizing like the OPC, is based on the principles of single particle elastic light scattering following the Mie theory (Rosenberg *et al.*, 2012). And then it is calibrated by a reference PSL (Polystyrene Latex Particle, Duke Scientific Corp., Palo Alto CA 94303, USA) to get a relationship between the response and the reference particle size. From the calibration results, the particle sizing of the BDS is divided by the size range of 0.23–25 μm in up to 32 bin sizes. Finally, it is calibrated with the reference equipment, APS3321 (TSI, MN55126, USA), using the reference PSL.

2.2 Measuring Fluorescence Efficiencies by Particle Sizes of the Test Samples

In order to investigate the capability of the BDS to measure fluorescence signals by particle sizes of the test samples, a set of instrument including a powder dispenser and a reference equipment was installed as shown in Fig. 2. First, The HEPA filter was installed on the BDS to prevent contaminated ambient air from entering the BDS. As the powder dispenser for particle generating of the test samples, small scale powder dispenser (SSPD) model 3433 (TSI Inc., St, Paul, MN, USA) was used and its flow rate is controlled by the flow regulator connected to the SSPD. After connecting the flow splitter 3708 (TSI Inc., St, Paul, MN, USA) to the outlet of the SSPD, one line of the flow splitter was connected to the nozzle of the BDS and the other to the nozzle of the APS3321, to provide the same sample to the both at the same time. The test samples was put on the surface of the SSPD turntable and gently brushed to be dispersed, and the turntable rotation speed was set at 1.5 rev/hr. After one

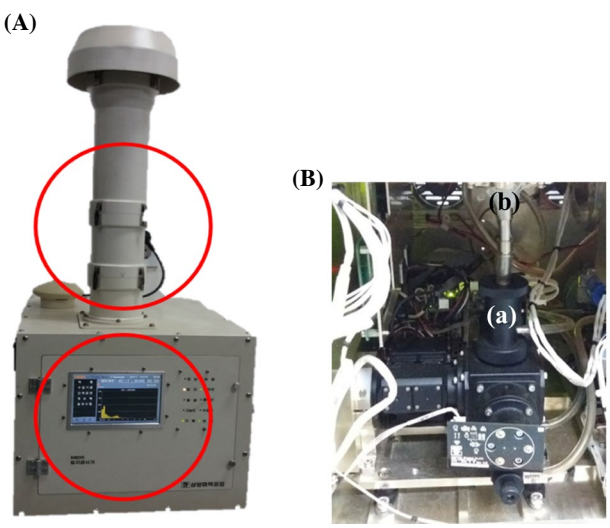

Fig. 1. Bio-aerosol Detection System (BDS): (A) External shape of the BDS with the concentration module (upper circle) and the monitoring module (lower circle), and (B) Inside of the monitoring module with the optical chamber (a) and the nozzle (b) into which the enriched particles enter the optical chamber.

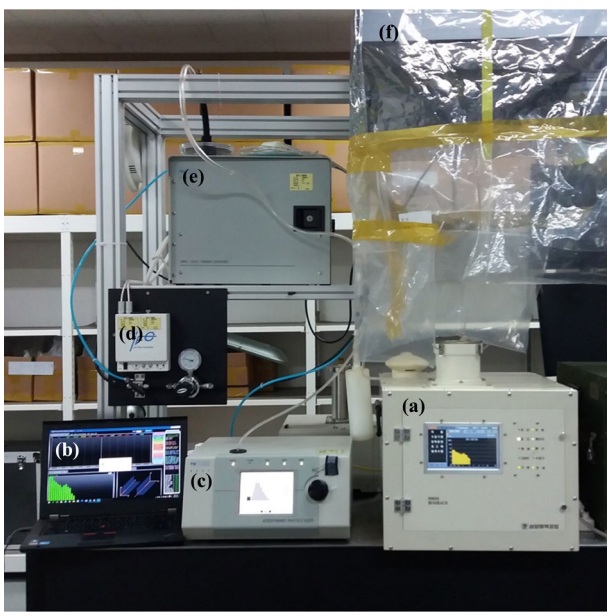

Fig. 2. Installing the BDS with the operating module under the HEPA filter to prevent contaminated air from entering into the BDS: the BDS (a), Operating module (b), APS3321 (c), Flow regulator (d), Small scale powder dispenser (SSPD) (e), and HEPA filter (f).

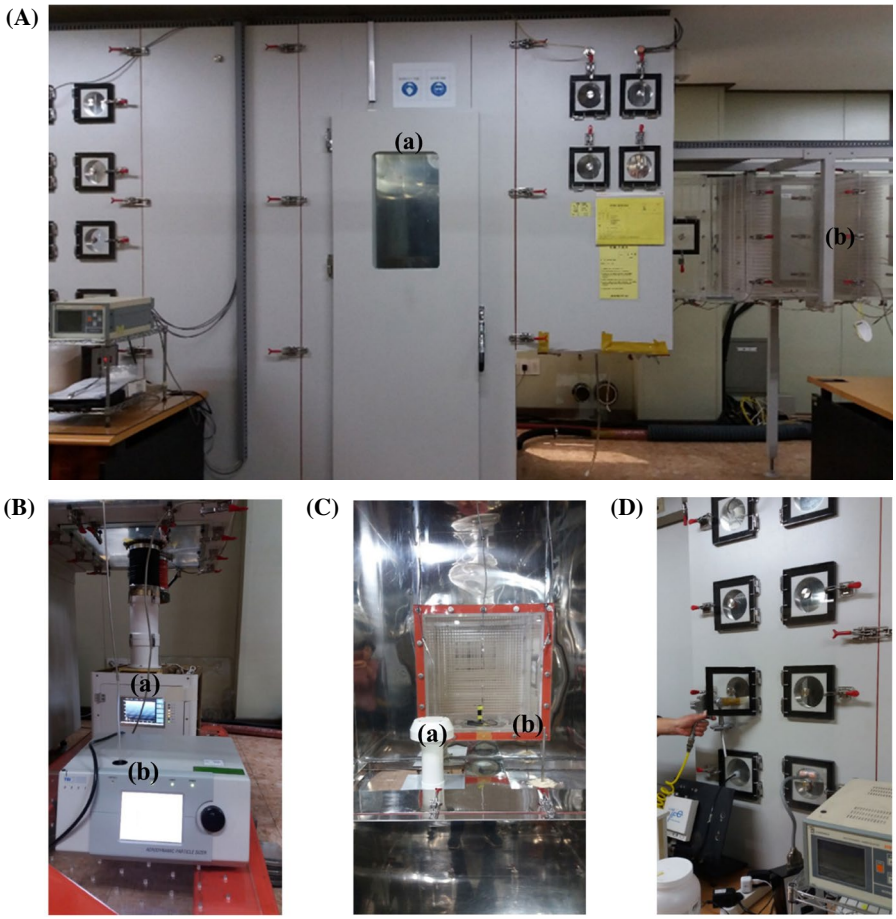

Fig. 3. Installing of the BDS and APS3321 into the wind tunnel linked with the aerosol chamber: (A) the aerosol chamber (a) with the wind tunnel (b), (B) the BDS (a) and APS3321 (b) at the bottom outside of the wind tunnel after installation, (C) the inlets of the BDS (a) and APS3321 (b) inside of the wind tunnel after installation, and (D) dspersing the test samples into the aerosol chamber using an air gun.

sample was tested, the turntable was replaced with a clean one, and after confirming with the APS3321 that the inside of the SSPD was clean, other sample was tested. The collected information was stored in the operating module for further analysis.

2.3 Real-time Monitoring of ND and IB Virus Vaccines

The BDS was located in the wind tunnel linked with the aerosol chamber. APS3321 was installed in the same way as the BDS (Fig. 3B, C). Before testing the samples, the BDS was calibrated for particle sizing using the APS3321 and PSLs (0.7–20 μm), and tested for blank using the test dust, SAE J726 (Powder technology Inc., WI 54476, USA). Next, after confirming with APS3321 that the aerosol chamber was clean, the test samples were then dispersed through the inlet of the aerosol chamber using an air gun, and the wind direction was set from the aerosol chamber to the wind tunnel (Fig. 3A). The fluorescence signals and the scattering signal of particles generated were measured as a function of time for real-time monitoring. In addition, to investigate the fluorescence efficiency depending on the concentration of each sample, ND was first dispersed with 4.3 mg, then with 0.5 mg after the aerosol chamber was cleaned. IB was also dispersed with 2.3 mg firstly, then the aerosol chamber was cleaned, followed by 1.5 mg.

2.4 Test Samples

PSLs (0.7 μm–20 μm) (Duke Scientific Corp., Palo Alto CA 94303, USA) were used for particle sizing calibration of the BDS and test dust, SAE J726 (Powder technology Inc., WI 54476, USA) for blank test. All the auto-fluorophores (Tryptophan, tyrosine, NADH, ribo-

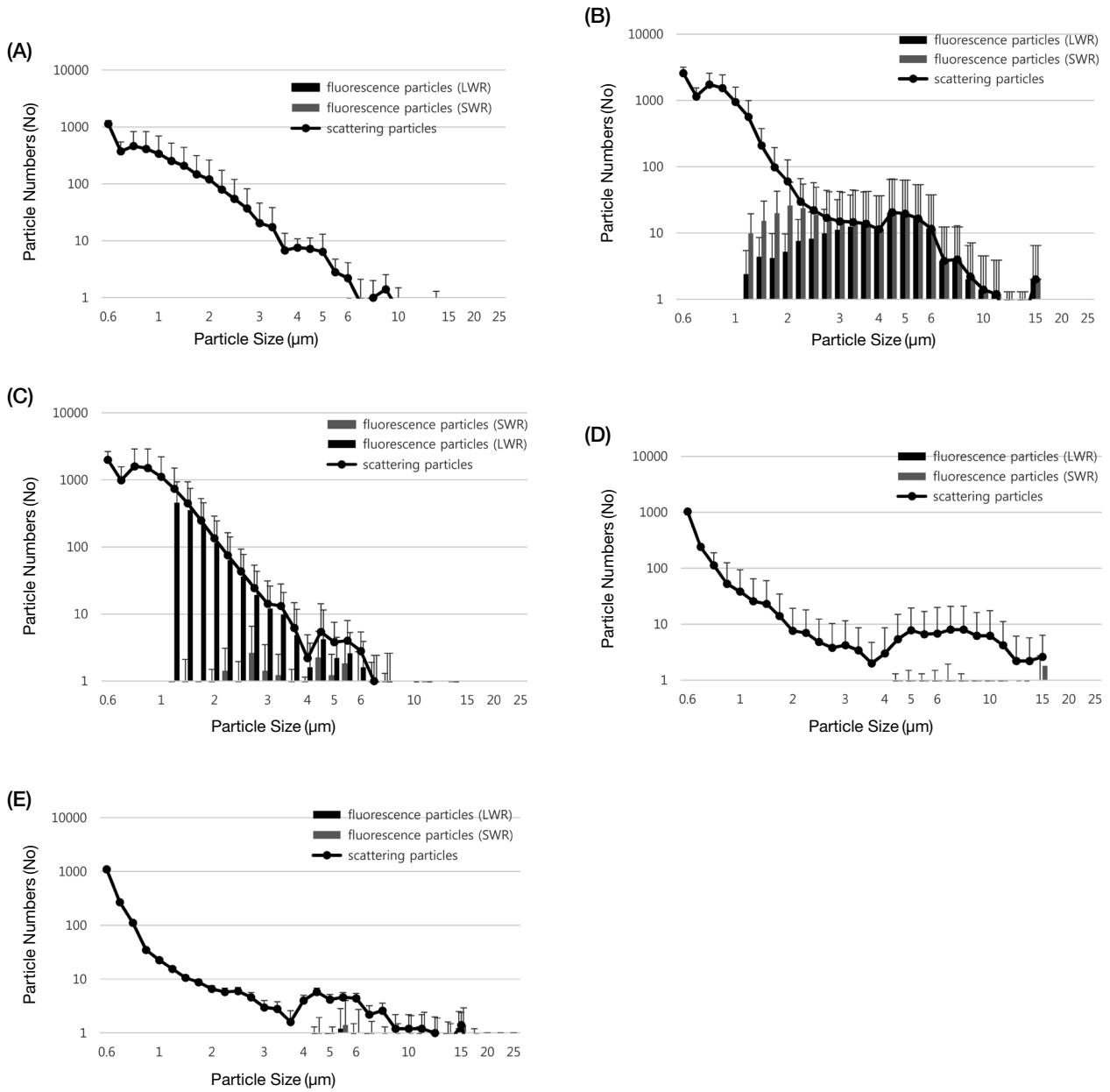

Fig. 4. The number of scattering particles (total particles) and fluorescence particles depending on the particle sizes of (A) J726, (B) NADH, (C) Riboflavin, (D) Tyrosine and (E) Tryptophan generated by SSPD.

flavin) were purchased from Sigma-Aldrich (St. Louis, Missouri, USA). ND vaccine (Merial S.A.S., Duluth-Georgia, USA) and IB vaccine (Daesung Microbiological Labs. Co., Ltd, Uiwang-si, Gyeonggi-do, Korea) were used as virus particle samples. Bacteriophage *MS2*, another virus simulant, was purchased from ATCC (VA 20110, USA), and directly propagated and lyophilized. *MS2* propagation is in accordance with the ATCC product sheet (ATCC® 15597-B1™). *Bacillus subtilis* as a representative bacterial strain was purchased from Bigbiogen (Anseong-si, Gyeonggi-do, Korea). All the test samples were powdered ones.

2.5 Data Analysis

The BDS data were analyzed using own developed analysis software. It processes the collected information every second. The information of individual particles includes scattered intensity classified as one of 32 bin

sizes so that determines the size of individual particles, and the fluorescence intensities of SWR (430–550 nm) and LWR (500–600 nm) classified as one of 16 bins determine whether or not it is a bio-particle. After combining the particle size information obtained from the scattering intensity and the fluorescence information according to each particle size, the numbers of bio-particles and non bio-particles by particle sizes was calculated. As mentioned in section 2.1, when the fluorescence signals are emitted simultaneously, they are measured as bio-particles, and when only scattered signals are emitted, as non bio-particles. It was consolidated in a spreadsheet (Microsoft Excel; Microsoft Corporation, Redmond, Washington, USA) and organized for statistical analysis. The experiments for fluorescence efficiencies by the particle sizes and monitoring ranges of the test samples, except for real-time monitoring, were carried out three times and averaged.

3. RESULTS

3.1 Fluorescence Efficiencies of NADH, Riboflavin, Tryptophan and Tyrosine

To investigate the scattering and fluorescence responses of the BDS on the particle size of auto-fluorophores, SSPD which is a system for generating aerosol by introducing powder, was used. As shown in Fig. 4A–E, the dispersed patterns were slightly different for each test sample but the dispersed size generally ranged from less than 1 to 15 μm. As expected, J726 showed almost no fluorescence particles in the entire dispersed particle size range. Among the auto-fluorophores, NADH and riboflavin showed fluorescence in the range of 1 μm or more, on the other hands, in tryptophan and tyrosine, as expected, fluorescence was scarcely observed over the entire particle size range. Regarding the fluorescence efficiencies, it was common in the both auto-fluorophores that the larger particle size, the higher the fluorescence efficiency (Fig. 5A). In the range of about 1 to 2 μm, the fluorescence efficiency of NADH was about 4 times higher in the SWR than in the LWR, and that of riboflavin was about 300 times higher in the LWR. In the range of >2 to 15 μm, the fluorescence efficiency of NADH was about 1.1 times higher in the SWR than in the LWR, and that of riboflavin was about 4 times higher in the LWR. Therefore, the general phenomenon is that the fluorescence efficiency of NADH was higher in the SWR and that of riboflavin in the LWR (Fig. 5B).

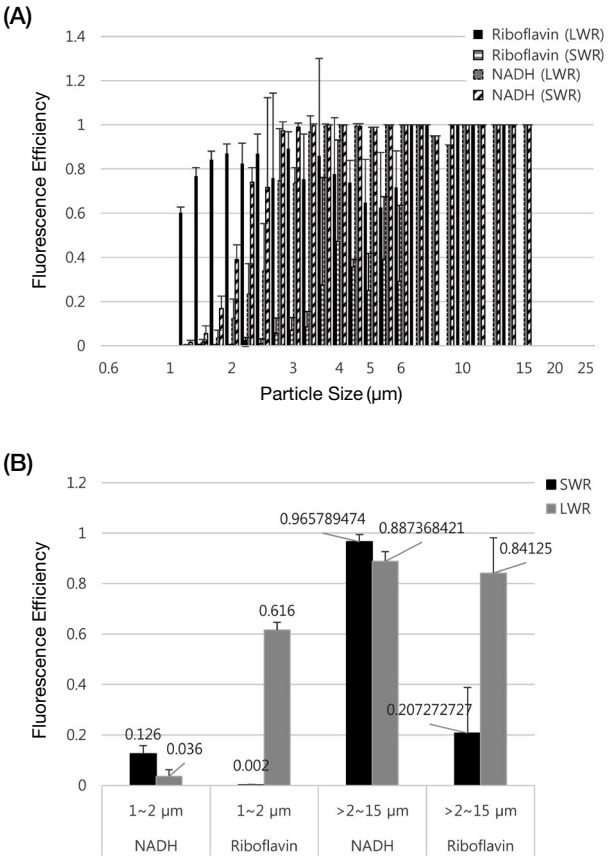

Fig. 5. Fluorescence efficiencies of NADH and riboflavin according to the two emission ranges (SWR: 430–550 nm, LWR: 500–600 nm): (A) by the generated particle sizes, (B) by the generated particle size ranges.

3.2 Fluorescence Efficiencies of ND, IB, *MS2* and *Bacillus subtilis* (BS)

The number distributions of scattering and fluorescence particles by particle sizes of the dispersed samples (ND, IB, *MS2* and BS) were shown in Fig. 6A–D. The distribution patterns were slightly different for each sample but the dispersed particle size generally ranged from less than 1 μm to 15 μm. As mentioned in section 2.1, the BDS measures as bio-particles when the two-fluorescence signals (in the SWR and in the LWR) are emitted simultaneously. Thus, by measuring the fluorescence signals and the scattering signals at the same time, the bio-particles can also be sized by the BDS. As shown in Fig. 6, the minimum particle size that the BDS can measure as bio-particles was more than approximately 2 μm in all the tested samples, although there were slight differences between the test samples. As shown in Fig. 7, the particle sizes of each sample exhibiting fluorescence efficiency of

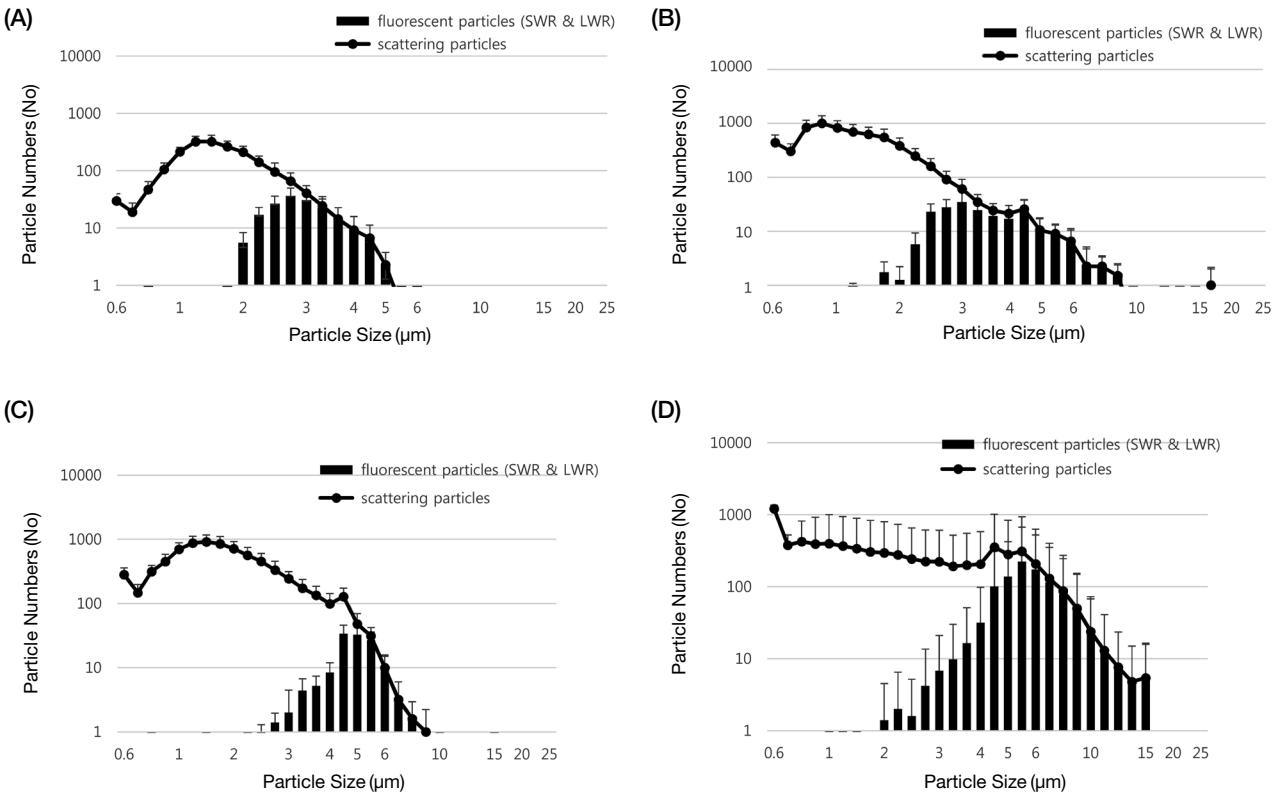

Fig. 6. The number distributions of scattering particles (total particles) and fluorescence particles emitting fluorescence in the SWR and in the LWR at the same time depending on the particle sizes of (A) ND, (B) BS, (C) IB and (D) *MS2* generated by SSPD.

more than 50% follows as: about 3 μm for ND and BS, about 5 μm for IB and *MS2*. The larger the size of the particles, the higher the fluorescence efficiency. This was also common as in the auto-fluorophores.

3.3 Real-time Monitoring Experiment

Experiment on real-time monitoring was performed by dispersing the test samples into the aerosol chamber using an air gun, where the samples used were ND and IB. The background particles were monitored with APS3321 each time before the sample tested, and the sample was injected when the background particles were less than 10. To exclude the false positive response of the BDS of detecting scattering particles as fluorescence particles, dust J726 was tested firstly. As the result, the false positive response was excluded because fluorescence particles were rarely observed (Fig. 8A). The number fluctuations of fluorescence particles and scattering particles as a function of time was shown in Fig. 8B, C. As the amount of generated particles increase, the number of fluorescence particles also increased in the both samples. As shown in Table 1, without dividing the particle size ranges, the ratios of the total fluorescence particles in the total scattering particles (the total fluorescence efficiencies) were 0.23 and 0.27 when dispersed with 4.3 mg and 0.5 mg of ND, respectively. And the total fluorescence efficiencies of IB were 0.09 and 0.086 when dis-

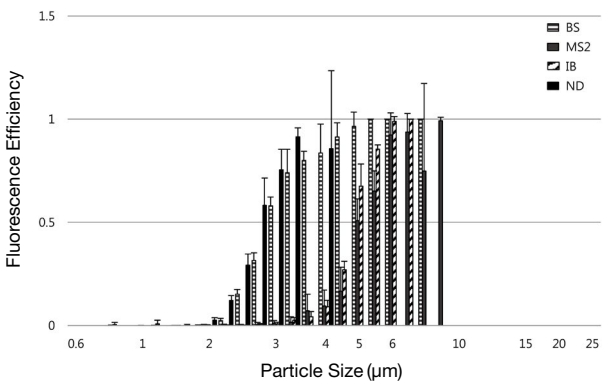

Fig. 7. Fluorescence efficiencies of ND, BS, IB and *MS2* depending on the particle sizes generated by SSPD.

Table 1. The concentration of total fluorescence particles and total scattering particles passing through the monitoring module of the BDS.

Dispersed amount (mg)	ND		IB	
	Scattering particles/Liter	Fluorescence particles/Liter	Scattering particles/Liter	Fluorescence particles/Liter
4.3	130	30	–	–
0.5	11	3	–	–
2.3	–	–	197	18
1.3	–	–	81	7

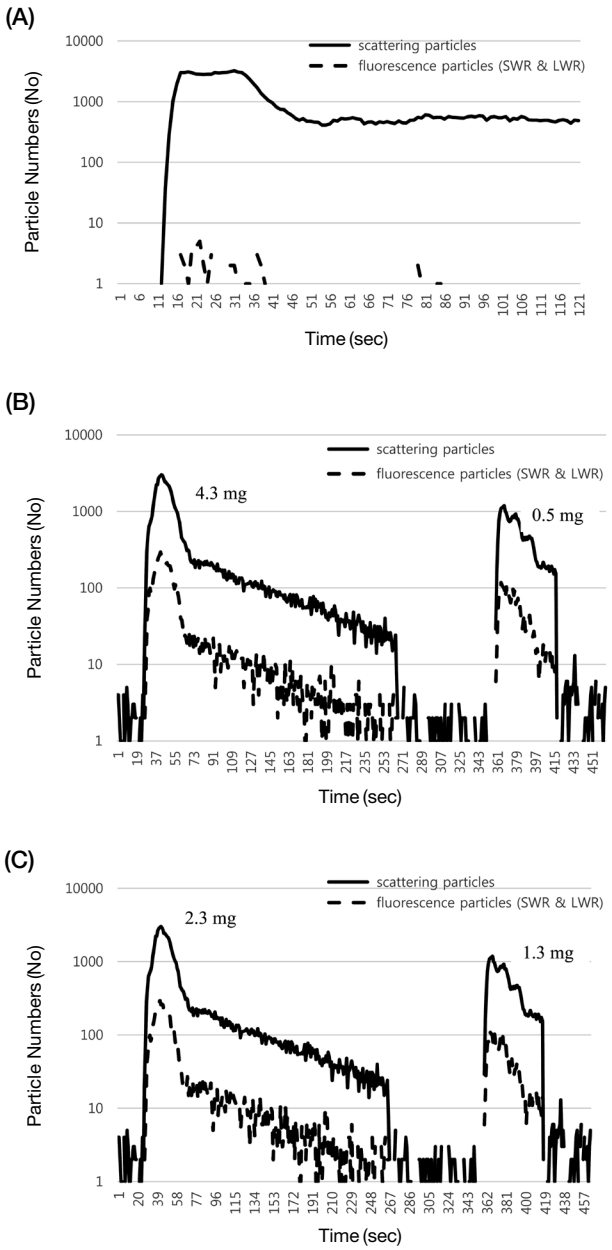

Fig. 8. The number distributions of scattering particles (total particles) and fluorescence particles of (A) J726, (B) ND and (C) IB as a function of time.

persed with 2.3 mg and 1.3 mg, respectively. Since particles smaller than 1 μm were included in the total fluorescence efficiencies, it was much lower than the fluorescence efficiencies in the particle size ranges mentioned in Section 3.2. Comparing the total fluorescence efficiencies depending on the dispersed amount, it did not changed much in the both samples, but there was a significant difference depending on the kind of samples, which the total fluorescence efficiency of ND was about 3 times higher than that of IB.

4. DISCUSSION

In order to evaluate the LIF-based BDS with 405 nm on real-time monitoring of aerosol particles including virus particles as well as bacteria, we have performed experiments in aerosol chambers using *Bacillus subtilis*, two kinds of virus vaccine (ND, IB) and bacteriophage *MS2*. First, we investigated the fluorescence response of the BDS on particle sizes of auto-fluorophores including NADH, riboflavin, tryptophan and tyrosine. As shown in Fig. 4, NADH and riboflavin exhibited fluorescence in the size ranges of 1 to 15 μm. On the other hands, tryptophan and tyrosine showed almost no fluorescence in all observed particle size ranges as expected. This is due to the nature of the auto-fluorophores, which rarely absorbs light at 405 nm (Pan, 2015). The absorption peaks of NADH generally ranges from 340 nm to 360 nm (Fennelly *et al.*, 2018). Nonetheless, in this study, NADH fluoresced by 405 nm. One reason is that NADH may absorb some wavelength of the incident light (405 nm) even though 405 nm is not within the absorption peak range of NADH (Hill *et al.*, 2013). Some also observed the fluorescence of NADH using the LIF-based BioScout with 405 nm, and reported that fluorescence efficiency is not only specific for biomolecules or biological particles, but also depends on equipment details such as the excitation source and the detection band (Saari *et al.*, 2014). As

shown in Fig. 5B, comparing the fluorescence efficiencies of auto-fluorophores depending on the particle size ranges, in the range of 1 to 2 μm, NADH was about 4 times higher in the SWR than in the LWR, and riboflavin was about 300 times higher in the LWR than in the SWR. Meanwhile, in the range of > 2 to 15 μm, NADH was about 1.1 times higher in the SWR than in the LWR, and riboflavin was about 4 times higher in the LWR than in the SWR. Overall, NADH was higher in the SWR than in the LWR and riboflavin was reversed. These results implies that the fluorescence monitoring of bio-particles containing NADH and riboflavin, which contribute to atmospherically relevant bio-aerosol fluorescence (Fennelly *et al.*, 2018), is possible by the LIF-based instrument with 405 nm. Moreover, the BDS measures them as bio-particles when the fluorescence signals from two wavelength ranges occur simultaneously so that it increases the accuracy of bio-particles rather than using one kind of fluorescence signal. However, individual viruses, which typically is not associated with NADH or riboflavin, commonly contain one or more of the fluorescing amino acids (tyrosine, tryptophan) will not fluoresce by 405 nm. Nonetheless, it may be assumed that the atmospheric virus particles, unlike individual viruses, may also fluoresce by 405 nm due to auto-fluorophores from a complex mixture of host respiratory track fluids, because they are discharged through the respiratory tract of their host (Reynolds and Chrétien, 1984). One reported the virus particles [VEE (*Venezuelan equine encephalitis TC83*), *MS2*] fluoresce by 405 nm, the reason is probably dominated by the fluorescence of the lysate of the host cells (Vero cells in the case of VEE, *E. coli* in the case of *MS2*) (Pan, 2015). Most virus vaccines are also dominated by the allantoic fluid of embryonated chicken eggs, the host used for the proliferation process (Brauer and Chen, 2015). Therefore, *MS2* or virus vaccine is considered to be more a suitable sample than individual virus particles for experiments on airborne virus particles. Thus, next, the possibility of monitoring airborne-virus particles using 405 nm was examined by using virus vaccines and bacteriophage *MS2*, virus simulant. As shown in Fig. 6, the aerosolized particle distribution pattern varied somewhat for each sample. But the number distribution of the fluorescence particles was similar, it ranged from approximately 2 to 15 μm in the tested samples, while the fluorescence efficiencies were different depending on the test samples. The fluorescence efficiencies were 70% at 3 μm for ND and BS, and 70% and 50% at 5 μm for IB and *MS2*, respectively. Thus, It was higher in ND and BS rather than in IB and *MS2* (Fig. 7). The difference in the fluorescence efficiency may be due to differences in the constituents from each sample production process. In the study, the aerosolized virus particle capable of fluorescence monitoring by the BDS ranges from 2 to 15 μm, which is considerably larger than individual virus particle ranging from several nm to several tens of nm. One demonstrated that more than one-half of the viral particles detected by PCR were within the respirable aerosol fraction (diameter, < 4 μm) (Blachere *et al.*, 2009). Moreover, the viability of viruses is reported to be particle size dependent. Some found that the viable IAV (Influenza A Virus) and PRRSV (Porcine Reproductive and Respiratory Syndrome Virus) can only be isolated from particles larger than 2.1 μm (Alonso *et al.*, 2015), and also demonstrated 93% recovery on aerosolized *MS2* of 2–5 μm using a novel growth tube collector (Pan *et al.*, 2016). This suggests that virus particles in the size range detectable (2–15 μm) by the LIF-based BDS using 405 nm may have high viability. Finally, for real-time monitoring, the samples was dispersed in the aerosol chamber. The results in Table 1 show the total fluorescence efficiency by indicating the concentration of the total fluorescence particles and the total scattering particles passing through the monitoring module without dividing the particle size ranges. The total fluorescence efficiency was no significant difference depending on the concentration, but there was significant difference depending on the samples by showing about 3 times higher in ND than in IB. This is thought to be a difference between the two vaccine components as mentioned above. Overall, despite the insensitivity of the BDS to tyrosine and tryptophan, and given the observed fluorescence efficiencies of bio-particles including virus particles with the BDS using 405 nm excitation light, it appears that this excitation wavelength may prove interesting in the continued development of instrumentation for the real-time monitoring of airborne-virus particles. In particular, it is not easy to predict the appearance of virus particles in the ambient environment. This is because it is not virus-specific and not easy to distinguish when the concentration of background bio-particles is high. Taken together, along with the fluorescence monitoring function of the LIF instrument with 405 nm, further development of algorithms to distinguish virus epidemic situation from normal background concentration will improve the capability of real-time monitoring of the BDS as the first responder in the field.

REFERENCES

Agranovski, V., Ristovski, Z., Hargreaves, M., Blackall, P.J., Morawska, L. (2003) Real-time measurement of bacterial aerosols with the uvaps: Performance evaluation. Journal of Aerosol Science 34(3), 301–317, DOI: 10.1016/S0021-8502(02)00181-7.

Agranovski, V., Ristovski, Z.D., Ayoko, G.A., Morawska, L. (2004) Performance evaluation of the uvaps in measuring biological aerosols: Fluorescence spectra from nad(p)h coenzymes and riboflavin. Aerosol Science and Technology 38(4), 354–364, DOI: 10.1080/02786820490437505.

Alonso, C., Goede, D.P., Morrison, R.B., Davies, P.R., Rovira, A., Marthaler, D.G., Torremorell, M. (2014) Evidence of infectivity of airborne porcine epidemic diarrhea virus and detection of airborne viral rna at long distances from infected herds. Veterinary Research 45, DOI: 10.1186/Preaccept-1744488495124325.

Alonso, C., Raynor, P.C., Davies, P.R., Torremorell, M. (2015) Concentration, size distribution, and infectivity of airborne particles carrying swine viruses. PLOS One 10(8), 12, DOI: 10.1371/journal.pone.0135675.

Blachere, F.M., Lindsley, W.G., Pearce, T.A., Anderson, S.E., Fisher, M., Khakoo, R., Meade, B.J., Lander, O., Davis, S., Thewlis, R.E., Celik, I., Chen, B.T., Beezhold, D.H. (2009) Measurement of airborne influenza virus in a hospital emergency department. Clinical Infectious Diseases 48(4), 438–440, DOI: 10.1086/596478.

Brauer, R., Chen, P. (2015) Influenza virus propagation in embryonated chicken eggs. Journal of Visualized Experiments 97, e52421, DOI: 10.3791/52421.

Choi, K., Ha, Y., Lee, H.K., Lee, J. (2014) Development of a biological aerosol detector using laser-induced fluorescence and a particle collection system. Instrumentation Science & Technology 42(2), 200–214.

Cowling, B.J., Ip, D.K.M., Fang, V.J., Suntarattiwong, P., Olsen, S.J., Levy, J., Uyeki, T.M., Leung, G.M., Peiris, J.S.M., Chotpitayasunondh, T., Nishiura, H., Simmerman, J.M. (2013) Aerosol transmission is an important mode of influenza a virus spread. Nature Communication 4, 12, DOI: 10.1038/ncomms2922.

Denoya, C. (2016) Real-time continuous microbiological monitoring. NEW DRUG DELIVERY METHODS: FROM CONCEPT TO PATIENT, 38.

Douwes, J., Thorne, P., Pearce, N., Heederik, D. (2003) Bioaerosol health effects and exposure assessment: Progress and prospects. The Annals of Occupational Hygiene 47(3), 187–200.

Fennelly, M.J., Sewell, G., Prentice, M.B., O'Connor, D.J., Sodeau, J.R. (2018) Review: The use of real-time fluorescence instrumentation to monitor ambient primary biological aerosol particles (pbap). Atmosphere 9(1), 39, DOI: 10.3390/atmos9010001.

Hill, S.C., Pan, Y.-L., Williamson, C., Santarpia, J.L., Hill, H.H. (2013) Fluorescence of bioaerosols: Mathematical model including primary fluorescing and absorbing molecules in bacteria. OPTICS EXPRESS 21(19), DOI: 10.1364/OE.21.022285.

Huffman, J.A., Treutlein, B., Pöschl, U. (2009) Fluorescent biological aerosol particle concentrations and size distributions measured with an ultraviolet aerodynamic particle sizer (uvaps) in central europe. Atmospheric Chemistry and Physics Discussions 9(4), 17705–17751, DOI: 10.5194/acpd-9-17705-2009.

II, A.J.P., Schwake, D.O., Marr, L.C. (2017) Ten question concerning the aerosolization and transmission of legionella in the built environment. Building and Environment 123, 684–695, DOI: 10.1016/j.buildenv2017.06.024.

Li, Y., Huang, X., Yu, I.T.S., Wong, T.W., Qian, H. (2004) Role of air distribution in sars transmission during the largest nosocominal outbreak in hong kong. Indoor Air 15, 83–95, DOI: 10.1111/j.1600-0668.2004.00317.

Pan, M., Eiguren-Fernandez, A., Hsieh, H., Afshar-Mohajer, N., Hering, S.V., Lednicky, J., Fan, Z.H., Wu, C.-Y. (2016) Efficient collection of viable virus aerosol through laminar-flow, water-based condensational particle growth. Journal of Applied Microbiology 120, 805–815, DOI: 10.1111/jam.13051.

Pan, Y.-L. (2015) Detection and characterization of biological and other organic-carbon aerosol particles in atmosphere using fluorescence. Journal of Quantitative Spectroscopy & Radiative Transfer 150, 12–35, DOI: 10.1016/j.jqsrt.2014.06.007.

Reynolds, H., Chrétien, J. (1984) Respiratory tract fluids: Analysis of content and contemporary use in understanding lung diseases. Diseaes-a-month 30(5), 1–103.

Rosenberg, P.D., Dean, A.R., Williams, P.I., Dorsey, J.R., Minikin, A., Pickering, M.A., Petzold, A. (2012) Particle sizing calibration with refractive index correction for light scattering optical particle counters and impacts upon pcasp and cdp data collected during the fennec campaign. Atmospheric Measurement Techniques 5(5), 1147–1163., DOI: 10.5194/amt-5-1147-2012.

Saari, S., Reponen, T., Keskinen, J. (2014) Performance of two fluorescence-based real-time bioaerosol detectors: Bioscout vs. Uvaps. Aerosol Science and Technology 48, 371–378, DOI: 10.1080/02786826.2013.877579.

Wei, K., Zou, Z., Zheng, Y., Li, J., Shen, F., Wu, C.Y., Wu, Y., Hu, M., Yao, M. (2016) Ambient bioaerosol particle dynamics observed during haze and sunny days in beijing. The Science of the Total Environment 550, 751–759, DOI: 10.1016/j.scitotenv.2016.01.137.

Yoon, S.N., Lee, J., Kim, D., Yoo, H.S., Min, K.Y., Kim, M.C. (2018) Analysis of correlation between atmospheric fluorescent particles and biomaterials. Asian Journal of Atmospheric Environment 12(4), 346–355, DOI: 10.5572/ajae.2018.12.4.346.